

## Hydrogen energy storage system originated from nitrogen oxides in flue gas

Momoko Watanabe, Shinji Kambara\*

Environmental and Renewable Energy Systems Division  
Graduate school of engineering, Gifu university, Gifu, Japan  
e-mail: kambara@gifu-u.ac.jp

### ABSTRACT

An innovative energy storage and carrier system has proposed from our recent researches. The system has three kind of chemical reactors, which are a HNO<sub>3</sub> production reactor, a NH<sub>3</sub> production reactor, and a H<sub>2</sub> production reactor. In this paper, we focused on characteristics of HNO<sub>3</sub> production originated from nitrogen oxides in flue gas. HNO<sub>3</sub> was produced by photochemical oxidation of nitric oxide (NO<sub>x</sub>) using vacuum ultraviolet irradiation of 172 nm wavelength. The HNO<sub>3</sub> production was affected by the flow rates of the model flue gas. It found that a high NO removal rate was obtained in the NO/O<sub>2</sub>/H<sub>2</sub>O/N<sub>2</sub> system. A maximum NO conversion to HNO<sub>3</sub> was 97.4%. The effect of the gap length on the reaction rate constant  $k$  on the NO conversion to enhance the HNO<sub>3</sub> production. The  $k$  was 0.193 s<sup>-1</sup> for the  $\phi$ 80 reactor, whereas the  $k$  increased to 0.658 s<sup>-1</sup> for the  $\phi$ 60 reactor.

### KEYWORDS

Hydrogen, Ammonia, NO<sub>x</sub>, HNO<sub>3</sub>, Vacuum ultraviolet, Storage, Energy carrier

### INTRODUCTION

The introduction of a hydrogen economy has been an available strategy to control crimate change when hydrogen is produced without CO<sub>2</sub> emission. However, use of hydrogen has a large energy loss for its transportation and physical storages [1, 2]. Ammonia is a hydrogen storage material that may solve several problems related to the hydrogen transportation and storage in a hydrogen economy [3]. Therefore, an energy carrier and storage system using ammonia has been proposed [4]. For example, a system consisting of the hydrogen production by electrolysis of water, ammonia synthesis from hydrogen, and the hydrogen generation from ammonia, is recognized as a hydrogen carrier and storage system without CO<sub>2</sub> emission. However, the efficiently ammonia synthesis is currently difficult, though some researches have been performed ammonia synthesis studies at a low temperature and pressure [5, 6].

We have been developed an original deNO<sub>x</sub> reactor using vacuum ultra violet (VUV) of 172 nm wavelength [7]. Recently, we found that nitric acid (HNO<sub>3</sub>) was easily produced from NO<sub>x</sub> by photochemical oxidation. HNO<sub>3</sub> is an available material for NH<sub>3</sub> production, because NH<sub>3</sub> can generate from HNO<sub>3</sub> by reduction at atmosphere pressure and a low temperature [8]. On the other hand, an original plasma membrane reactor for H<sub>2</sub> production from ammonia also has been developed [9]. Using the plasma membrane reactor, pure hydrogen production for fuel cells was attained the flow rate of 21 L/h. These results have created a new hydrogen energy storage and carrier system consisting of the HNO<sub>3</sub> production reactor, the NH<sub>3</sub> production reactor, and the H<sub>2</sub> production reactor as shown in **Figure 1**. The advantage of this system is to combine deNO<sub>x</sub> without ammonia. Selective catalytic reduction (SCR) has been usually used for various combustors to remove NO<sub>x</sub>, which needs catalysts and ammonia for deNO<sub>x</sub>. If the energy system

shown in Figure 1 installs to the combustors, the cost of catalyst and ammonia would be reduced. Furthermore, excess electricity of renewable energy can use to drive each reactor; therefore hydrogen may be able to inexpensively produce. It is important for the establishment of this system to achieve high energy efficiency in each reactor.

In this paper, we focused on characteristics of  $\text{HNO}_3$  production. The present study aimed to investigate fundamental characteristics of the  $\text{HNO}_3$  production using the photochemical reactor. The effects of the flow rates and the chemical composition on  $\text{HNO}_3$  production using VUV was examined. Furthermore the effect of the gap length in the reactor on the NO conversion to  $\text{HNO}_3$  for an enhancement of the  $\text{HNO}_3$  production.

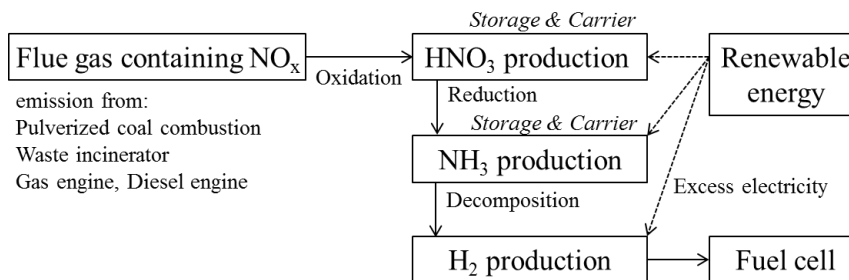


Figure 1. A proposal of a new hydrogen energy storage and carrier system

## EXPERIMENTAL APPARATUS AND METHOD

The experimental setup is shown in **Figure 2**. The apparatus consists of the gas mixing and flow control systems, the humidifier, the photochemical reactor, and the gas analysers. In experiments for  $\text{HNO}_3$  production, an  $\text{N}_2/\text{Air}$  gas mixture was prepared using the mass-flow controllers (MFCs) and the gas blender, and after then, moisture and NO gas were mixed. The  $\text{NO}/\text{O}_2/\text{H}_2\text{O}/\text{N}_2$  gas mixture was fed into the photochemical reactor as the model flue gas. The gas temperature depended on a  $\text{H}_2\text{O}$  concentration in the humidifier, which was varied from  $30\text{ }^\circ\text{C}$  to  $60\text{ }^\circ\text{C}$ . The temperature of a gas feed pipe maintained above the temperature of the humidifier by a line heater because of prevention of  $\text{H}_2\text{O}$  condensation in the pipe.

The photochemical reactor (inner diameter: 80 mm) was had a coaxial configuration with the excimer lamp (outer diameter: 40 mm; USHIO Inc.). A dielectric-barrier discharge (DBD) plasma unit using xenon gas was installed as part of the excimer lamp. When a high voltage was applied to an electrode of the DBD by the AC power source, Xe atoms were excited by the electron energy from the DBD plasma, and excited Xe atoms were returned instantaneously to their ground states. In this process, a narrow wavelength distribution having a peak intensity at 172 nm was continuously emitted. The model flue gas was fed into the gap between the excimer lamp and the inside wall of the cylindrical reactor. The gap volume was  $377\text{ cm}^3$ . The radiation power was  $26\text{ mW}\cdot\text{cm}^{-2}$  on the quartz glass surface of the excimer lamp. The pressure of the reactor was controlled to be slightly above atmospheric pressure using a gas sampler (SHIMAZU CFP-8000), which featured suction pumps and gas coolers. The gas composition of the output stream was continuously measured by gas analysers for NO,  $\text{NO}_2$  (HORIBA VIA510),  $\text{O}_2$  (SHIMAZU NOA-7000), and  $\text{N}_2\text{O}$  (HORIBA VIA510).

**Table 1** details the experimental conditions for  $\text{HNO}_3$  production. The total flow rate of the model flue gas was varied from  $1.0$  to  $5.0\text{ L min}^{-1}$ , and a NO concentration in the model gas was fixed 1500 ppm on dry basis. The  $\text{O}_2$  concentration and the  $\text{H}_2\text{O}$  partial pressure as saturated vapour pressure were changed as listed in Table 1.

The temperature of the model gas was heated to approximately  $150\text{ }^\circ\text{C}$  in the photochemical reactor by radiation of joule heating from the excimer lamp surface; moisture in the gas did not

condensed on the wall of the reactor. The power consumption of the excimer lamp at the plug was 90 W.

In all experimental conditions, the concentration of HNO<sub>3</sub> produced by the photochemical reaction was determined. The produced gas was introduced to the absorbing solution by switching the valves, and HNO<sub>3</sub> was completely recovered. The concentration of nitrate ion (NO<sub>3</sub><sup>-</sup>) in the solution was measured by the ion analyser (Toa-DKK IA-300).

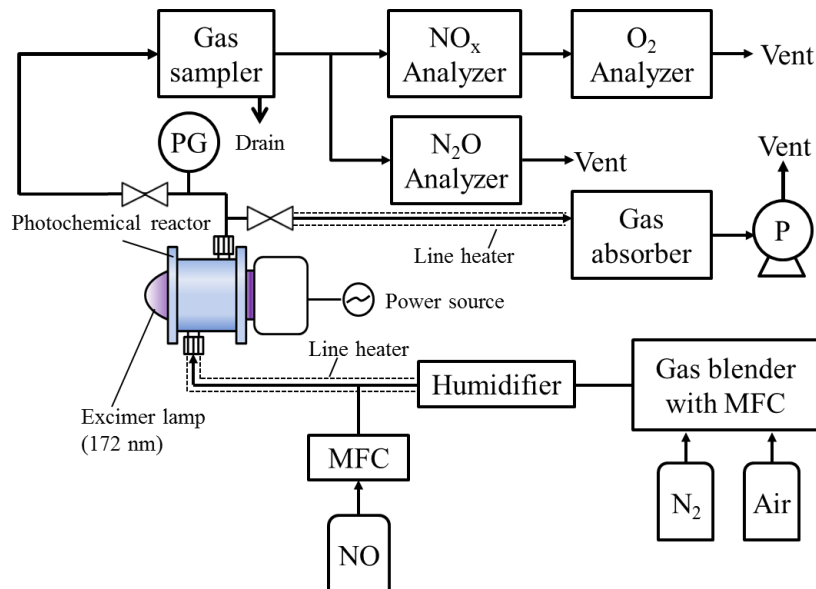


Figure 2 Experimental setup for HNO<sub>3</sub> production using VUV of 172 nm wavelength

Table 1 Experimental conditions for HNO<sub>3</sub> production

Total flow rate of model gas [L/min]	1.0–5.0
NO concentration [ppm, dry]	1500
O <sub>2</sub> concentration [% , dry]	0, 8.3
H <sub>2</sub> O partial pressure [kPa]	0–9.5

## RESULTS AND DISCUSSION

### Fundamental characteristics of HNO<sub>3</sub> production

**Figure 3** shows the effect of the flow rates of the NO/O<sub>2</sub>/H<sub>2</sub>O/N<sub>2</sub> gas mixture on the NO conversion to HNO<sub>3</sub>. The NO conversion to HNO<sub>3</sub> was calculated from the NO removal rate as follows:

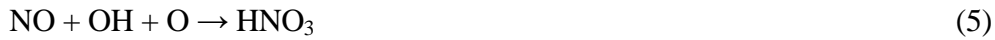
$$\text{NO removal rate [\%]} = ([\text{NO}]_{\text{IN}} - [\text{NO}_x]_{\text{OUT}}) / [\text{NO}]_{\text{IN}} \times 100 \quad (1)$$

$$\text{NO conversion to HNO}_3 \text{ [\%]} = \text{NO removal rate [\%]} \quad (2)$$

where [NO]<sub>IN</sub> is the initial NO concentration (1500 ppm by volume) and [NO<sub>x</sub>]<sub>OUT</sub> is the total concentration of NO, NO<sub>2</sub>, N<sub>2</sub>O (ppm, dry) in the gas produced by the photochemical reactor. However, in the NO/O<sub>2</sub>/H<sub>2</sub>O/N<sub>2</sub> gas mixture experiments, NO<sub>2</sub> and N<sub>2</sub>O was not detected. Furthermore the output mass of N was agreed with that of the input mass; therefore, Eq.2 is correct in the NO/O<sub>2</sub>/H<sub>2</sub>O/N<sub>2</sub> gas mixture experiments.

The NO conversion to HNO<sub>3</sub> was attained 97.4% at the flow rate of 1.0 L min<sup>-1</sup>, while it was decreased with an increase in the flow rate of the NO/O<sub>2</sub>/H<sub>2</sub>O/N<sub>2</sub> gas mixture. The each chemical

composition absorbs the light of 172 nm wavelength [10], and occurs various reactions. For example, the below reactions may concern:



where  $h$  is Planck constant, and  $\nu$  is frequency which is given by  $c/\lambda$  ( $c$  is the speed of light, and  $\lambda$  is wavelength).

In general, the reaction rate in the gas phase reaction such as Eq. (5) depends on the reaction time or gas residence time in the reactor. Therefore, the NO conversion to HNO<sub>3</sub> was affected by the flow rates.

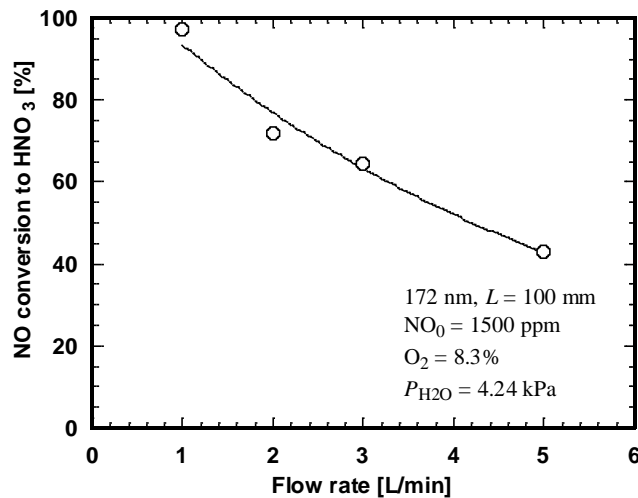


Figure 3. Variation in NO conversion rate to HNO<sub>3</sub> with flow rate of the model gas

#### • Reaction paths of HNO<sub>3</sub> production

To find effective reaction paths of the HNO<sub>3</sub> production, the four systems were examined as follows:

- 1) NO/N<sub>2</sub>
- 2) NO/H<sub>2</sub>O/N<sub>2</sub>
- 3) NO/O<sub>2</sub>/N<sub>2</sub>
- 4) NO/O<sub>2</sub>/H<sub>2</sub>O/N<sub>2</sub>

**Figure 4** shows the effect of gas composition on the NO removal rate as a function of the partial pressure of H<sub>2</sub>O. It found that high NO removal rate was obtained at the NO/O<sub>2</sub>/H<sub>2</sub>O/N<sub>2</sub> system only. Both O<sub>2</sub> and H<sub>2</sub>O were necessary for a high NO conversion to HNO<sub>3</sub>. In particular, the partial pressure of H<sub>2</sub>O was needed above 4.24 kPa for efficiency HNO<sub>3</sub> production in the experimental conditions.

In the NO/O<sub>2</sub>/H<sub>2</sub>O/N<sub>2</sub> system, the reactions relating to the HNO<sub>3</sub> production were considered as follows:



In fact, the generation of ozone was detected by qualitative analysis of ozone at the photochemical reactor exit. The issue on the enhancement of HNO<sub>3</sub> production is to find

rate-controlling step among Eqs.(3)–(8), but the kinetic reaction study will be conducted in future.

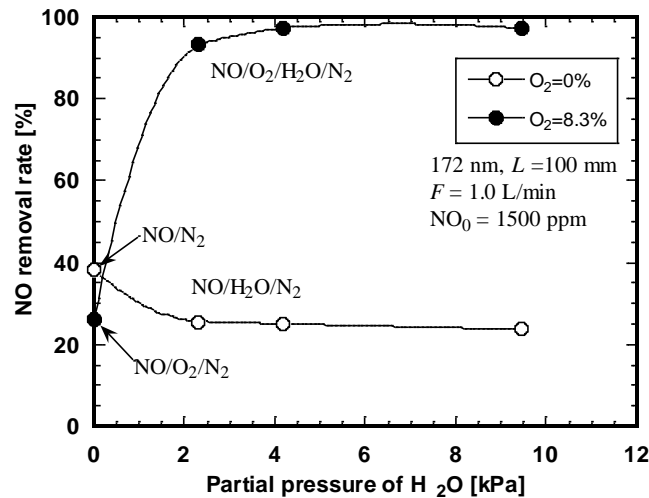


Figure 5. Effects of  $P_{\text{H}_2\text{O}}$  and gas composition on NO conversion to  $\text{HNO}_3$

#### • Enhancement of $\text{HNO}_3$ production

An efficiently VUV absorption of molecules is important for the enhancement of the  $\text{HNO}_3$  production. The photon energy  $h\nu$  is attenuated toward the inner wall in the photochemical reactor; therefore the gap length (or inner diameter of the reactor) affects the NO conversion to  $\text{HNO}_3$ .

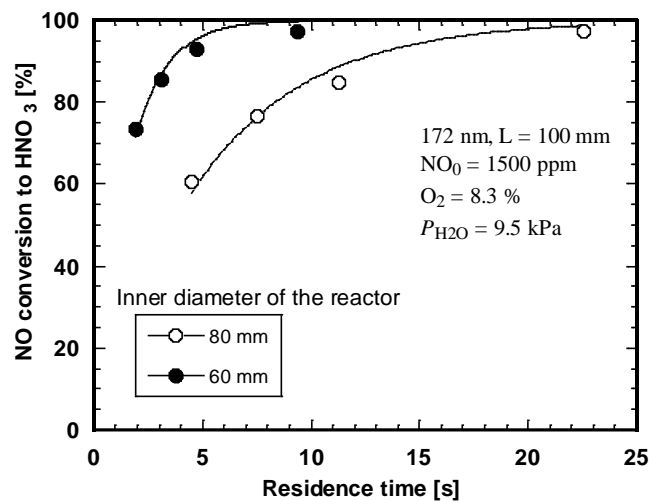


Figure 5. Effects of  $P_{\text{H}_2\text{O}}$  and gas composition on NO conversion to  $\text{HNO}_3$

To investigate the effect of the gap length, the photochemical reactor having an inner diameter of 60 mm was prepared. **Figure 5** shows variation in the NO conversion to  $\text{HNO}_3$  with an increase in gas residence time as a parameter of the inner diameter of the reactor. The gap length of the  $\phi 60$  reactor and the  $\phi 80$  reactor was 10 and 20 mm, respectively. The NO conversion to  $\text{HNO}_3$  enhanced using the photochemical reactor having the narrow gap length, even though gas residence time was short. This is because that molecular  $\text{H}_2\text{O}$  and  $\text{O}_2$  were effectively absorbed the VUV of the 172 nm wavelength in the narrow space.

The reaction rate of the  $\text{HNO}_3$  production assumes first-order reaction:

$$dX/dt = k X \quad (9)$$

$$X = 100 \times (1 - \exp(-k t)) \quad (10)$$

where  $X$  is NO conversion to  $\text{HNO}_3$  [%],  $t$  is gas residence time [s], and  $k$  is rate constant [ $\text{s}^{-1}$ ].

The solid line in Figure 5 is the fitting line by Eq.(10). The  $k$  was  $0.193 \text{ s}^{-1}$  for the  $\phi 80$  reactor, whereas the  $k$  was  $0.658 \text{ s}^{-1}$  for the  $\phi 60$  reactor. The  $k$  was enhanced 3.4 times in the narrow gap length.

## CONCLUSION

A new hydrogen energy storage and system consisting of the  $\text{HNO}_3$  production reactor, the  $\text{NH}_3$  production reactor, and the  $\text{H}_2$  production reactor has proposed from the recent research results. In this paper, the fundamental characteristics of the NO conversion to  $\text{HNO}_3$  using photochemical reactor with vacuum ultraviolet irradiation of 172 nm wavelength.

The  $\text{HNO}_3$  production was affected by the flow rates and the chemical composition of the model flue gas. The maximum  $\text{HNO}_3$  production was 97.4% in the  $\text{NO}/\text{O}_2/\text{H}_2\text{O}/\text{N}_2$  system.  $\text{O}_2$  and  $\text{H}_2\text{O}$  were necessary for the  $\text{HNO}_3$  production, and the partial pressure of  $\text{H}_2\text{O}$  was needed above 4.24 kPa for efficiently  $\text{HNO}_3$  production.

To enhance the  $\text{HNO}_3$  production, the effect of the gap length on the reaction rate constant  $k$  was examined. The NO conversion to  $\text{HNO}_3$  increased using the photochemical reactor having the narrow gap length, even though gas residence time was short. The  $k$  was  $0.193 \text{ s}^{-1}$  for the  $\phi 80$  reactor, whereas the  $k$  increased to  $0.658 \text{ s}^{-1}$  for the  $\phi 60$  reactor.

## ACKNOWLEDGMENT

## REFERENCES

1. Eberle U, Felderhoff M, Schueth F., Chemical and physical solutions for hydrogen storage, *Angew Chem. Int. Edit.*, Vol.48, 6608–6630, 2009.
2. Lan, R, Irvine, J. T. S. and Tao, S., Ammonia and Related Chemicals as Potential Indirect Hydrogen Storage Materials, *Int. J. Hydrogen Energy*, Vol. 37, No. 2, pp 1482-1494, 2012.
3. Green Jr L., An ammonia energy vector for the hydrogen economy, *Int. J. Hydrogen Energy*, Vol.35, 355–359, 1982.
4. Kojima Y., *J. Jpn. Inst. Energy*, Vol.93 No.5, pp.378–385, 2014. (in Japanese)
5. Pickett C.J., Talarmin J., Electrosynthesis of ammonia, *Nature*, Vol.317, 652–653, 1985.
6. Skodra A., Stoukides M., Electrocatalytic synthesis of ammonia from steam and nitrogen at atmospheric pressure, *Solid State Ionics*, Vol.180, 1332–1336, 2009.
7. Kambara S., Hayakawa Y., Masui M., Hishinuma N., Kumabe K., Moritomi H., Removal of nitric oxide by activated ammonia generated by vacuum ultraviolet radiation, *Fuel*, Vol.94, pp.274–279, 2012.
8. Crumpton W. G., Isenhardt T. M., Hersh C. M., Determination of Nitrate in Water Using Ammonia Probes and Reduction by Titanium (III), *Water Pollution Control Federation*, Vol. 59, No. 10, pp. 905–908, 1987.
9. Kambara S., Hayakawa Y., Inoue Y., Tomonori M., Hydrogen production from ammonia by a plasma membrane reactor, *J. Sustainable Dev. Energy, Water & Env. Systems*, to be submitted.
10. Thompson B. A., Harteck P., Reeves Jr R. R., Ultraviolet absorption coefficients of  $\text{CO}_2$ ,  $\text{CO}$ ,  $\text{O}_2$ ,  $\text{H}_2\text{O}$ ,  $\text{N}_2\text{O}$ ,  $\text{NH}_3$ ,  $\text{NO}$ ,  $\text{SO}_2$ , and  $\text{CH}_4$  between 1850 and 4000 Å, *J Geophysical Res.*, Vol.68, No.24, pp.6431–6436, 1963.